Electronic supplementary information

The generalized Debye model for $\chi_{ac}(\omega)$, $\omega = 2\pi f$ taking into account two relaxation paths (processes).

$$\chi'(\omega) = \chi_{FR} + \frac{\chi_{SR1}\left[1 + (\omega\tau_1)^{1-\alpha_1}\sin 1/2\alpha_1\pi\right]}{1 + 2(\omega\tau_1)^{1-\alpha_1}\sin 1/2\alpha_1\pi + (\omega\tau_1)^{2(1-\alpha_1)}} + \frac{\chi_{SR2}\left[1 + (\omega\tau_2)^{1-\alpha_2}\sin 1/2\alpha_2\pi\right]}{1 + 2(\omega\tau_2)^{1-\alpha_2}\sin 1/2\alpha_2\pi + (\omega\tau_2)^{2(1-\alpha_2)}},$$

$$\chi''(\omega) = \frac{\chi_{SR1}(\omega\tau_1)^{1-\alpha_1}\cos 1/2\alpha_1\pi}{1 + 2(\omega\tau_1)^{1-\alpha_1}\sin 1/2\alpha_1\pi + (\omega\tau_1)^{2(1-\alpha_1)}} + \frac{\chi_{SR2}(\omega\tau_2)^{1-\alpha_2}\cos 1/2\alpha_2\pi}{1 + 2(\omega\tau_2)^{1-\alpha_2}\sin 1/2\alpha_2\pi + (\omega\tau_2)^{2(1-\alpha_2)}}.$$

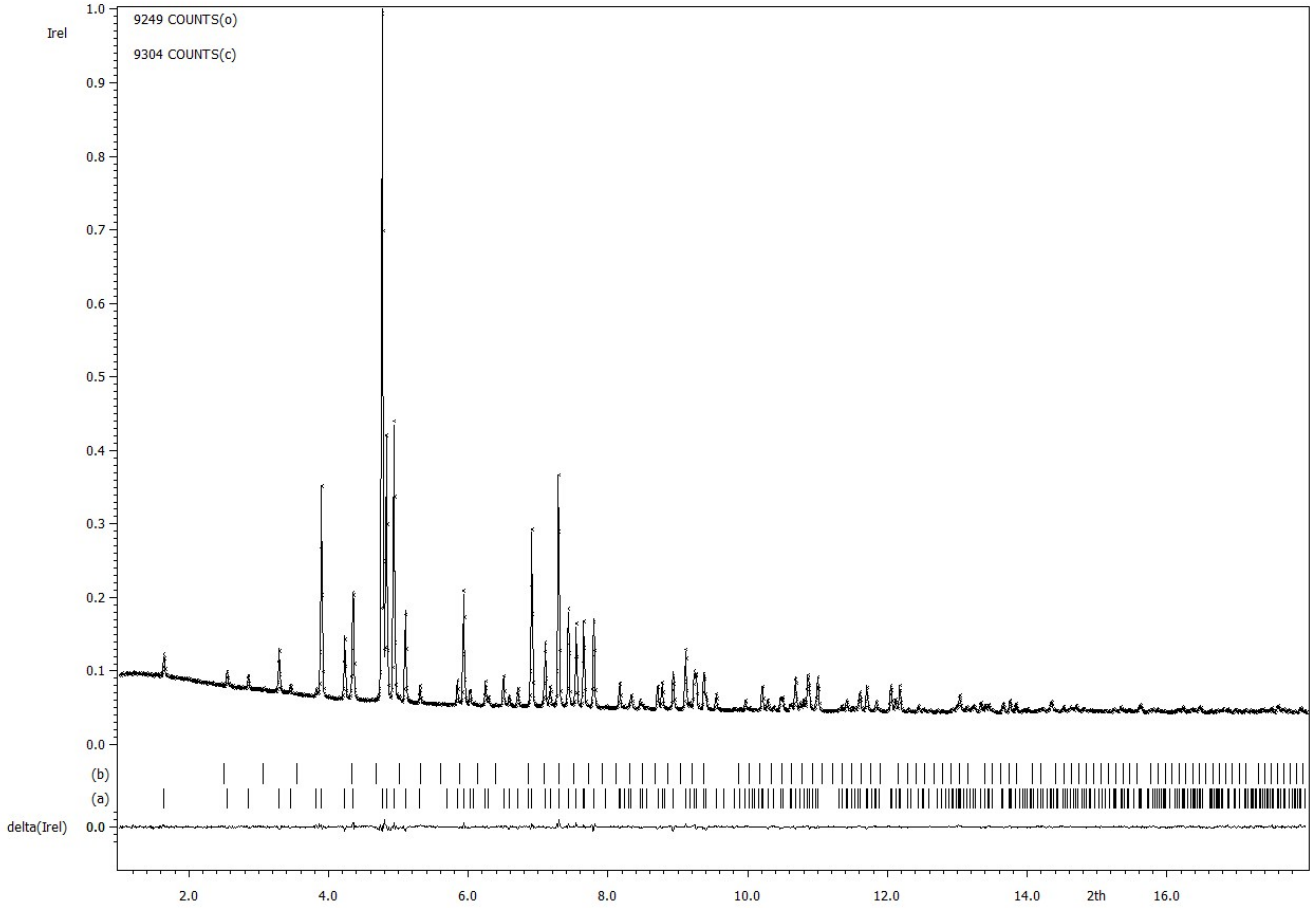

Figure S1. Synchrotron powder X-ray diffraction pattern of $Ca_{9.5}Tb_{0.5}(PO_4)_6(OH_{0.75-\delta})_2$. Observed (crosses), calculated (solid line) and difference (solid line below) plots. Positions of Bragg reflections are shown as strokes underneath. (a) the main apatite phase, (b) the trace of Tb_4O_7 (0.4 wt. %).

Table S1. Crystal structure refinement data for $Ca_{9.5}Tb_{0.5}(PO_4)_6(OH_{0.75-\delta})_2$.[a)]

Temperature (K)	293 K
Wavelength (Å)	0.23369
Space group	$P6_3/m$
a (Å)	9.4001(1)
c (Å)	6.8744(1)
V (Å^3)	526.05(1)
Z	1
2θ range (deg.)	1 – 18
R_{wp}	0.015
R_{all}	0.037
ΔF_{max}, ΔF_{min} (e Å^{-3})	0.36, -0.44

[a)]Further details of the crystal structure investigations may be obtained from the Fachinformationszentrum Karlsruhe, 76344 Eggenstein-Leopoldshafen, Germany (Fax: +49-7247-808-666; E-Mail: crysdata@fizkarlsruhe.de, http://www.fiz-karlsruhe.de/request for deposited data.html) on quoting the depository number CSD 433685 or from the Cambridge Database, CCDC 1857532.

Table S2. Atomic parameters and thermal displacement parameters (Å^2) for $Ca_{9.5}Tb_{0.5}(PO_4)_6(OH_{0.75-\delta})_2$.

Atom[a]	Ca(1)	Ca(2)[b]	P	O(1)	O(2)	O(3)	O(4)	Tb
Site	4f	6h	6h	6h	6h	12i	4e	6h
SOF	1	0.918(2)	1	1	1	1	0.471(6)	0.082(2)
x	1/3	0.0105(7)	0.3982(3)	0.3289(5)	0.5846(7)	0.3422(4)	0	0.004(2)
y	2/3	0.2538(5)	0.3696(3)	0.4852(6)	0.4614(7)	0.2586(4)	0	0.2253(17)
z	0.0005(5)	1/4	1/4	1/4	1/4	0.0685(4)	0.1851(14)	1/4
U_{eq}, U_{iso}	0.0239(8)	0.0197(7)	0.0229(15)	0.0131(17)	0.0322(19)	0.0309(14)	0.032(4)	0.0197(7)
U_{11}	0.0220(10)		0.0248(19)					
U_{22}	0.0220(10)		0.023(2)					
U_{33}	0.0275(15)		0.0125(16)					
U_{12}	0.0110(5)		0.0060(15)					
U_{13}	0		0					
U_{23}	0		0					

[a] Hydrogen atoms were not determined in the structure. The hydrogen content was calculated to get electroneutrality, δ was introduced to take into account a possible O_2^{2-} formation.

[b] The sum of the Ca(2) and Tb site occupancies was fixed to 1 and U_{iso} of Ca(2) and Tb was constrained to be equal.

Table S3. Selected interatomic distances (Å) and angles (degrees) in the crystal structure of $Ca_{9.5}Tb_{0.5}(PO_4)_6(OH_{0.75-\delta})_2$.

Ca(1)-O(1)	2.404(5)	3x	O(1)-P-O(2)	112.2(4)	
Ca(1)-O(2)	2.437(6)	3x	O(1)-P-O(3)	111.1(2)	2x
Ca(1)-O(3)	2.807(5)	3x	O(2)-P-O(3)	107.0(3)	2x
Ca(2)-O(1)	2.680(6)		O(3)-P-O(3)	108.2(2)	
Ca(2)-O(2)	2.407(12)		O(1)-Tb-O(3)	69.2(3)	2x
Ca(2)-O(3)	2.321(3)	2x	O(3)-Tb-O(3)	77.6(3)	2x
Ca(2)-O(3)	2.543(6)	2x	O(3)-Tb-O(3)	60.5(5)	
Ca(2)-O(4)	2.380(6)		O(1)-Tb-O(2)	94.4(5)	
Tb-O(1)	2.801(16)		O(2)-Tb-O(3)	80.2(5)	2x
Tb-O(2)	2.60(3)		O(2)-Tb-O(3)	72.1(7)	2x
Tb-O(3)	2.396(6)	2x	O(1)-Tb-O(4)	109.5(9)	
Tb-O(3)	2.476(17)	2x	O(3)-Tb-O(4)	96.3(5)	
Tb-O(4)	2.15(2)		O(3)-Tb-O(4)	81.0(4)	
P-O(1)	1.521(7)		O(3)-Tb-O(4)	93.1(5)	
P-O(2)	1.517(6)		O(3)-Tb-O(4)	119.3(8)	
P-O(3)	1.541(4)	2x	O(2)-Tb-O(4)	153.1(8)	

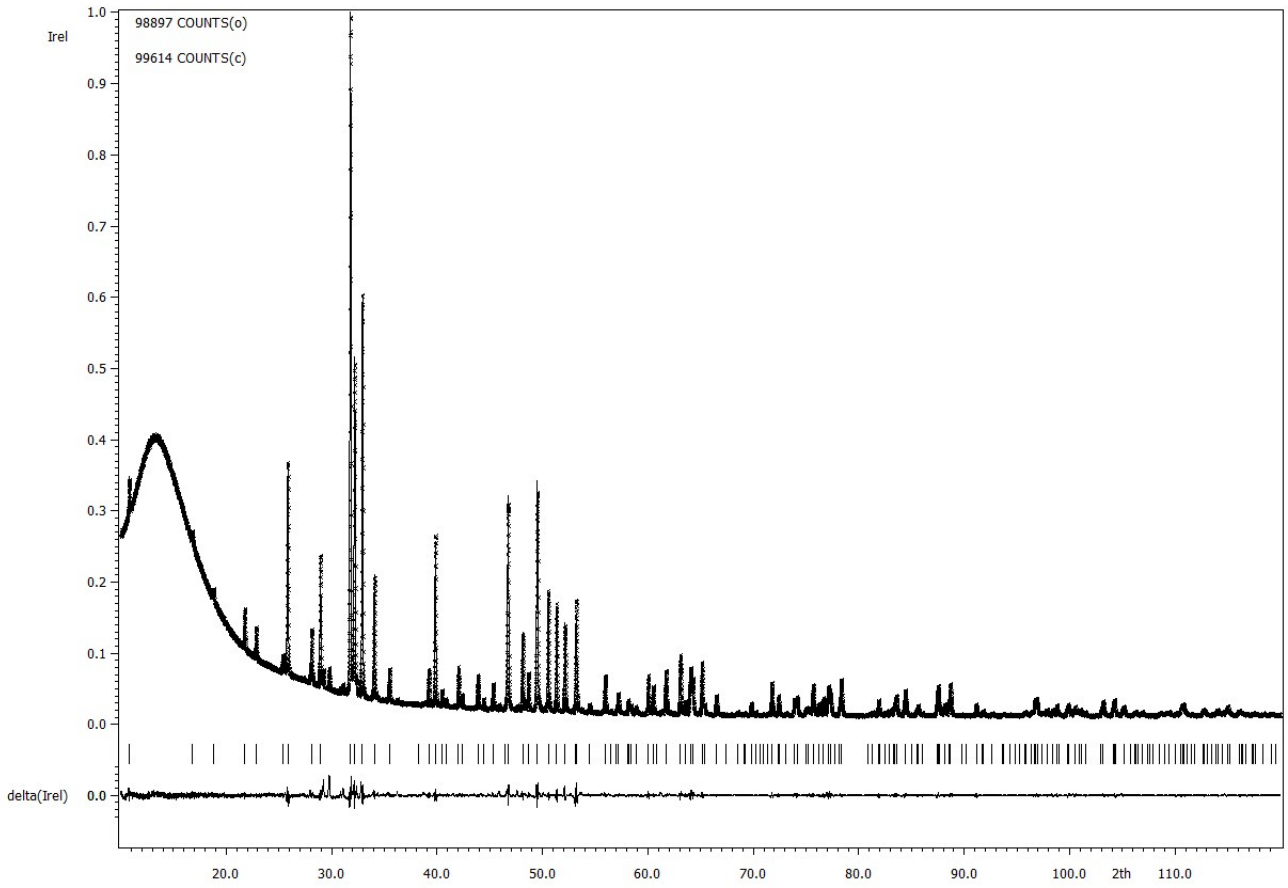

Figure S2. X-ray diffraction pattern of $Ca_{9.9}Tb_{0.1}(PO_4)_6(OH_{0.95-\delta})_2$. Observed (crosses), calculated (solid line) and difference (solid line below) plots. Profile fitting only. Positions of Bragg reflections are shown as strokes underneath.

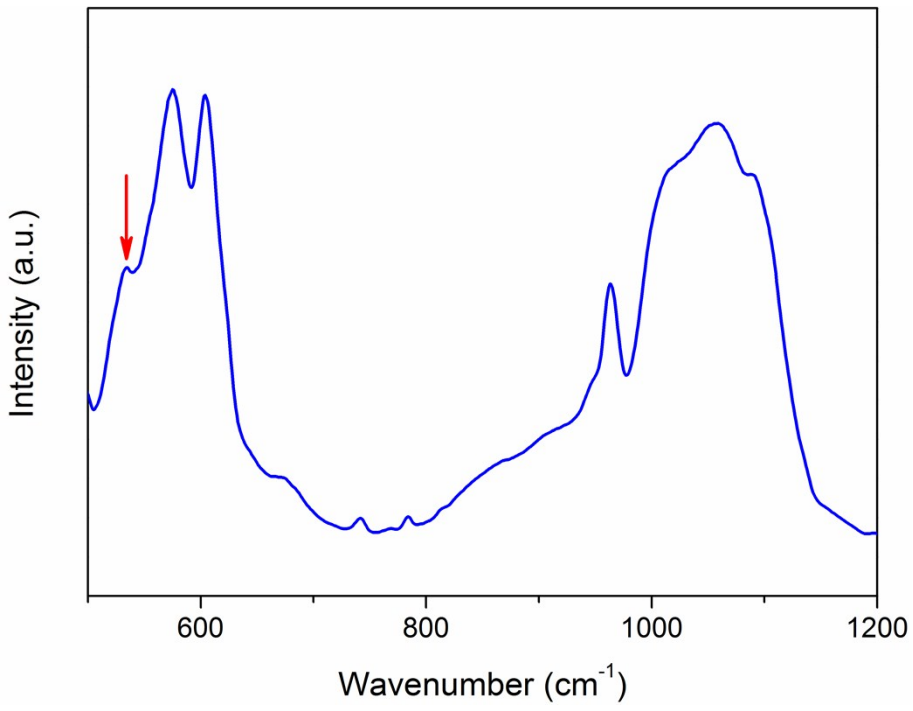

Figure S3. FT-IR spectra of $Ca_{9.5}Tb_{0.5}(PO_4)_6(OH_{0.75-\delta})_2$. The peak of the Tb-O valent vibration is marked with the arrow.

Table S4. Crystal field parameters derived in the program CONCORD for Tb^{3+} using experimental atomic coordinates of the coordination polyhedron (from Table S2). Partial charges on the phosphate oxygen atoms and on the intrachannel oxygen atom are -0.4567 and -0.9134 respectively.

Parameter	Value (cm^{-1})
B_{20}	1376.7437
B_{22}	-78.37187
B_{40}	205.66633
B_{42}	73.86198
B_{43}	5.15638
B_{44}	-12.86961
B_{60}	30.12361
B_{62}	8.86534
B_{63}	6.68935
B_{64}	4.84489
B_{66}	-9.72317
B_{21}	-71.78134
B_{41}	-145.37119
B_{61}	-33.78635
B_{65}	1.82679
B_{21}'	30.64804
B_{22}'	-0.44207
B_{41}'	61.26934
B_{42}'	-61.80919
B_{43}'	14.83528
B_{44}'	8.77577
B_{61}'	5.78564
B_{62}'	-0.53062
B_{63}'	8.92765
B_{64}'	0.66326
B_{65}'	3.49962
B_{66}'	3.65152

Table S5. Modeling with the program CONCORD using crystal field parameters listed in Table S4. Energies of first 49 energy levels of Tb^{3+} under a zero field and their (negative) magnetic moments under a field of 1 kOe for spins antiparallel (odd row) and parallel (even row) to the magnetic field. .

Energy (cm^{-1})	μ_z (μ_B)	μ_x (μ_B)	μ_y (μ_B)
0	-8.957	-0.0034	-0.01363
1.391E-4	8.957	-0.00339	0.00544
177.5	-7.357	-0.3527	-0.1881
177.5	7.357	0.3463	0.1811
345.8	-5.599	-0.221	-0.05686
346	5.599	0.2144	0.0499
497.6	-0.9434	-0.02673	-0.01012
499.3	0.9433	0.01831	3.633E-4
620.6	-0.0928	3.498E-5	-0.021
628.1	0.09232	-0.01912	-0.00245
696.2	-0.0051	0.03525	-0.02122
730.8	0.00339	-0.3022	0.0139
748	0.00217	0.314	0.06231
2211	-7.51	-0.8038	-0.3741
2211	7.51	0.7944	0.3648
2334	-5.746	-0.00796	-0.00723
2335	5.746	-0.00178	-0.00451
2431	-0.5255	-0.01659	-0.01356
2434	0.5254	0.00343	-0.0103
2493	-0.07637	0.00213	-0.06805
2501	0.07464	-0.05473	0.00623
2522	-0.00363	0.07803	0.05259
2564	-0.00115	-1.89	0.00186
2567	0.00628	1.896	0.05172
3697	-1.963	-0.3137	-0.3282
3698	1.617	0.1803	0.2019
3701	0.306	0.04585	-0.2472
3706	-0.00746	-0.01338	0.3261
3718	0.02184	0.02382	-0.07063
3733	-0.8336	-0.04726	-0.05998
3734	0.7612	0.00406	0.07706
3741	-0.2684	-0.9482	0.04749
3742	0.3662	1.068	0.05304
4603	-2.773E-4	-0.02478	-0.03695
4632	-0.02144	-0.00638	0.03182
4640	0.02124	0.01831	-0.00603
4716	-0.1804	0.00362	0.00347
4721	0.1806	0.00365	0.00231
4852	-3.844	-0.01898	-0.00265
4852	3.844	0.02426	0.00767
5211	-2.658E-4	-0.00243	-0.00261
5341	-0.01018	0.00165	-0.00113
5364	0.01039	-0.00122	0.00228
5619	-0.1925	-2.747E-4	-3.947E-5
5624	0.1885	0.00212	6.814E-4
5666	0.00464	4.252E-4	0.00102
6057	-0.01099	6.774E-4	-0.00242
6087	0.01136	-0.00341	7.702E-4
6220	3.29E-4	0.00386	0.00295

Table S6. Energies of first 49 energy levels of Tb^{3+} under a zero field and their (negative) magnetic moments under a field of 1 kOe for spins antiparallel (odd row) and parallel (even row) to the magnetic field obtained after the fitting the experimental spectrum of luminescence by the variation of the parameters B_{20}, B_{40}, and B_{22} keeping all other B-parameters at the values listed in Table S4. Fitted values of B_{20}, B_{40}, and B_{22} are 1250, 550, and -350 cm^{-1} respectively.

Energy (cm^{-1})	μ_z (μ_B)	μ_x (μ_B)	μ_y (μ_B)
0	-8.898	-0.01736	-0.05344
0.01132	8.898	0.00938	0.03668
111.7	-6.961	-0.05375	-0.04431
112	6.961	0.04805	0.03937
247.3	-1.145	-0.00864	-0.00747
249.9	1.144	0.00378	7.187E-4
377.7	-0.075	0.00537	-0.01336
397.6	0.07395	-0.0167	8.754E-4
479	-0.00748	0.02439	0.00168
555.5	0.00659	-0.1428	0.00543
582.5	-1.066E-4	0.1472	0.01935
747.3	-0.00627	-2.102	0.00525
750.5	0.00881	2.102	0.00885
2131	-7.502	-0.5238	-0.2981
2131	7.502	0.517	0.2904
2290	-4.26	-0.01555	-0.01694
2290	4.259	0.00578	-0.01258
2348	-0.02858	0.0079	-0.2074
2364	-9.998E-4	-0.07066	0.2125
2380	0.01174	0.0769	-0.00515
2434	0.00752	-0.286	0.00722
2445	0.00432	0.2877	0.01721
2539	0.00119	-5.958	0.00497
2539	0.00539	5.958	0.00746
3603	-0.3105	-0.01443	-0.5639
3606	-0.09074	-0.04692	0.347
3609	-0.06864	0.0357	-0.039
3612	0.4588	-0.00988	0.238
3657	-0.02861	0.01625	-0.07491
3673	-0.06328	-0.1935	0.0716
3678	0.06636	0.2075	0.00575
3708	0.0186	-0.3911	0.00355
3714	0.01767	0.3961	0.01154
4566	-0.00148	-0.04949	-0.1705
4574	-0.02025	-0.0132	0.1656
4582	0.02056	0.04566	-0.00852
4631	-0.04174	0.00584	0.00713
4649	0.0424	0.00439	0.00182
4767	-0.7515	0.00152	0.00134
4770	0.7517	0.00504	0.00271
5209	-5.895E-4	-0.01042	-0.00678
5238	-0.00338	0.01001	-5.343E-4
5292	0.00374	-0.00209	0.00645
5500	-0.01849	0.00198	9.169E-5
5539	0.01585	7.163E-4	3.482E-4
5659	0.00349	1.8E-4	3.947E-4
5934	-0.00212	6.197E-4	-0.00104
6077	0.0025	-0.00621	8.708E-4
6167	4.101E-4	0.00647	0.00182

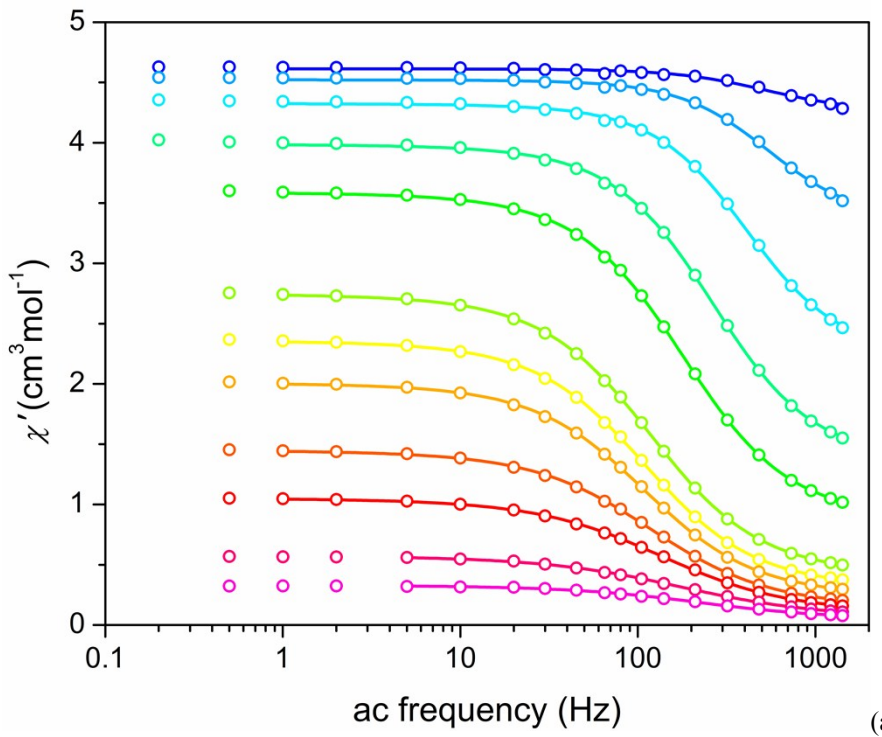

(a)

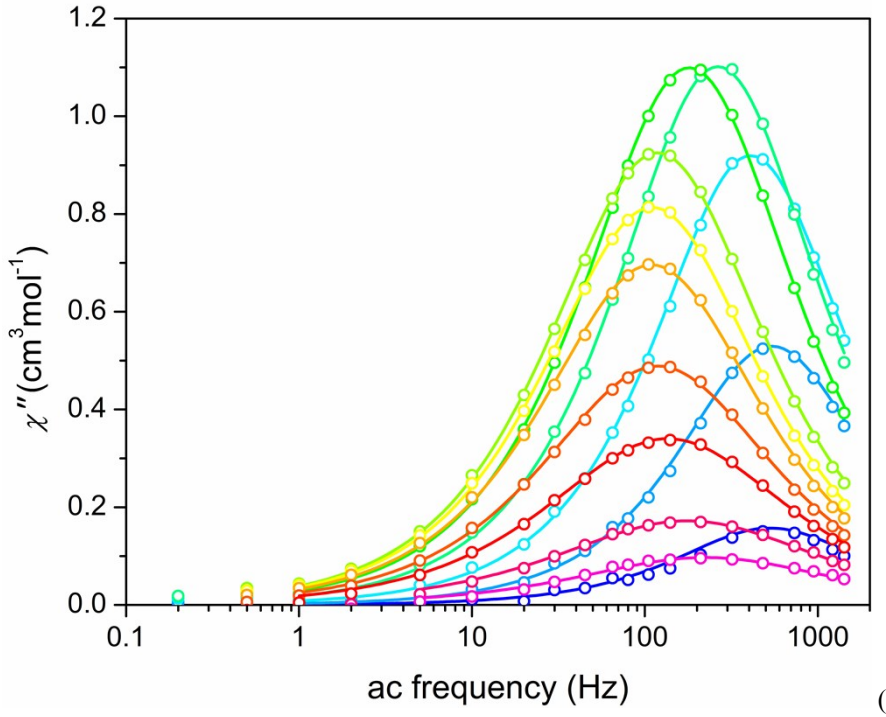

(b)

Figure S4. Frequency dependence of ac susceptibility per mol of Tb for $Ca_{9.9}Tb_{0.1}(PO_4)_6(OH_{0.95-\delta})_2$ under different magnetic fields at T = 1.8 K. (a) – in-phase susceptibility χ', (b) – out-of-phase susceptibility χ''. Symbols – experimental points, lines – fitting. The color designation: from blue to magenta – under a field of 0.3, 0.6, 1, 1.5, 2, 3, 3.5, 4, 5, 6, 8, 10 kOe respectively.

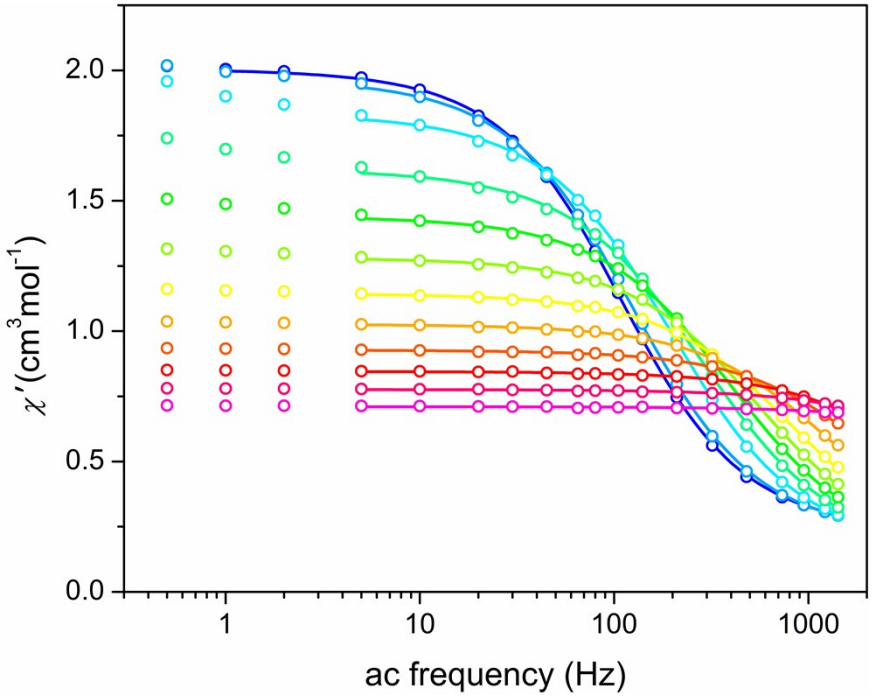

(a)

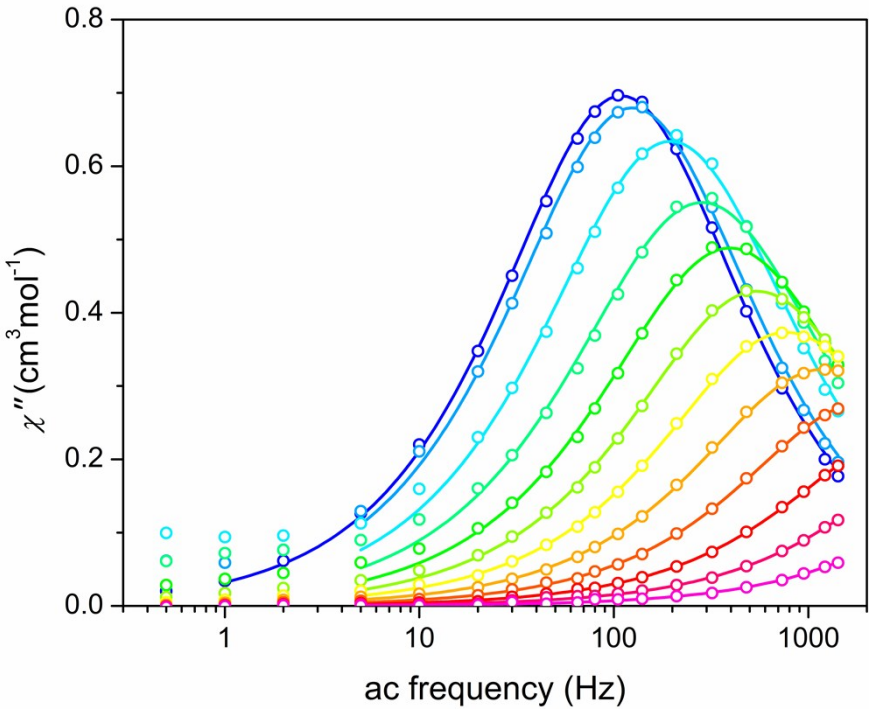

(b)

Figure S5. Frequency dependence of ac susceptibility per mol of Tb for $Ca_{9.9}Tb_{0.1}(PO_4)_6(OH_{0.95-\delta})_2$ at different temperatures under a field of 4 kOe. (a) – in-phase susceptibility χ', (b) – out-of-phase susceptibility χ''. Symbols – experimental points, lines – fitting. The color designation: from blue to magenta – at T = 1.8, 2, 3, 4, 5, 6, 7, 8, 9, 10, 11, 12 K respectively.

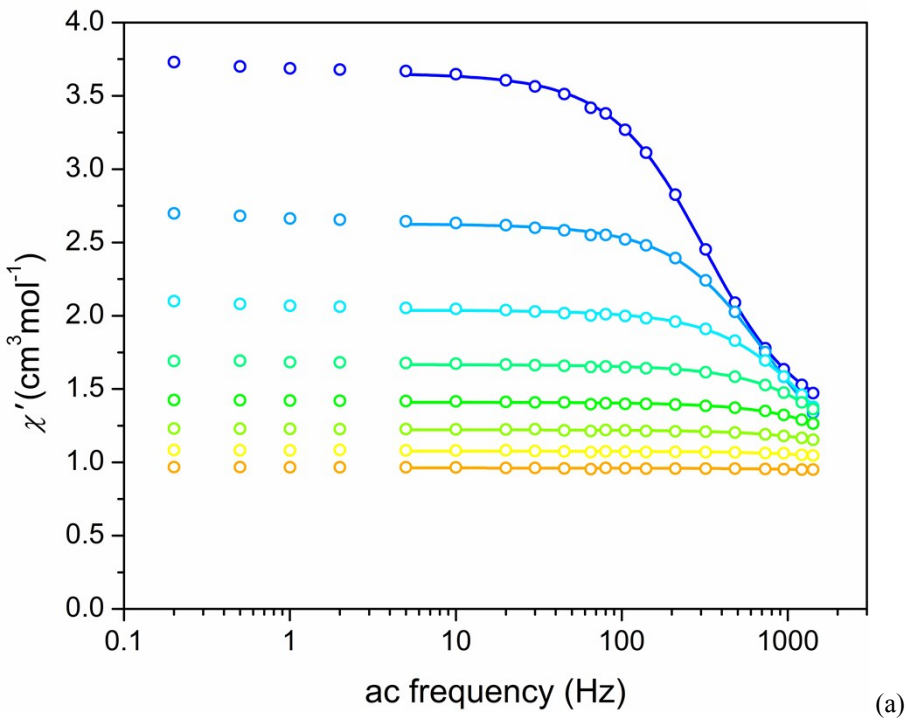

(a)

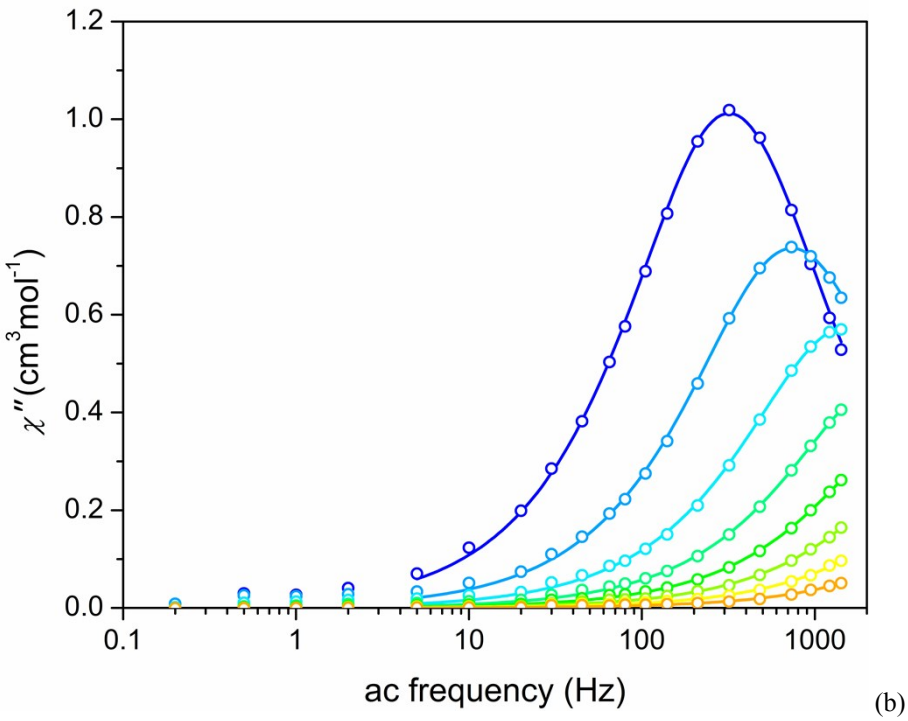

(b)

Figure S6. Frequency dependence of ac susceptibility per mol of Tb for $Ca_{9.9}Tb_{0.1}(PO_4)_6(OH_{0.95-\delta})_2$ at different temperatures under a field of 1.5 kOe. (a) – in-phase susceptibility χ', (b) – out-of-phase susceptibility χ''. Symbols – experimental points, lines – fitting. The color designation: from blue to magenta – at T = 2, 3, 4, 5, 6, 7, 8, 9 K respectively.

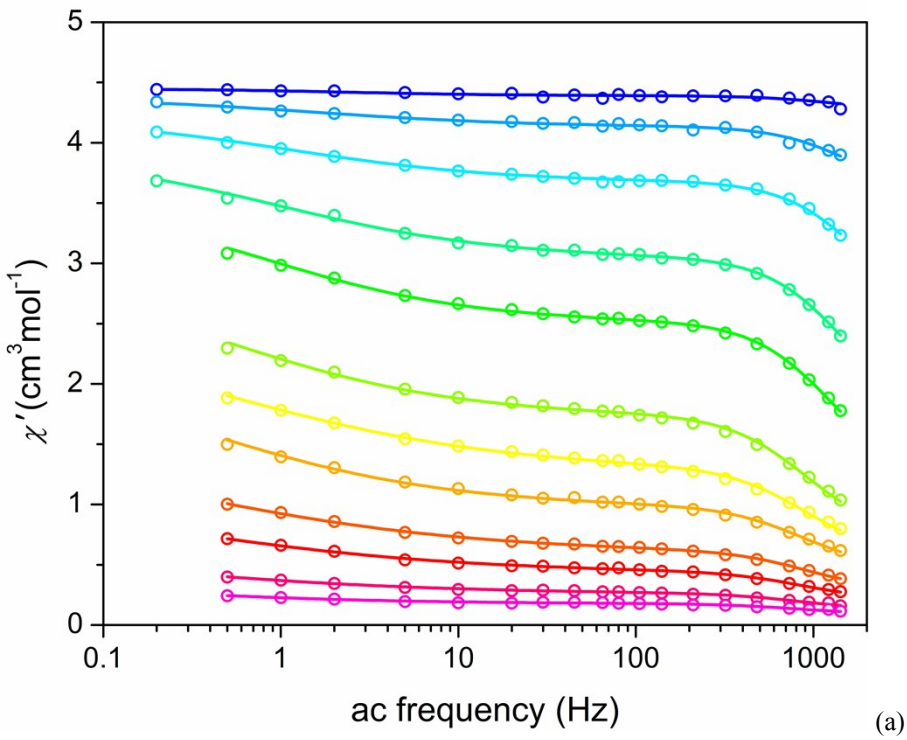

(a)

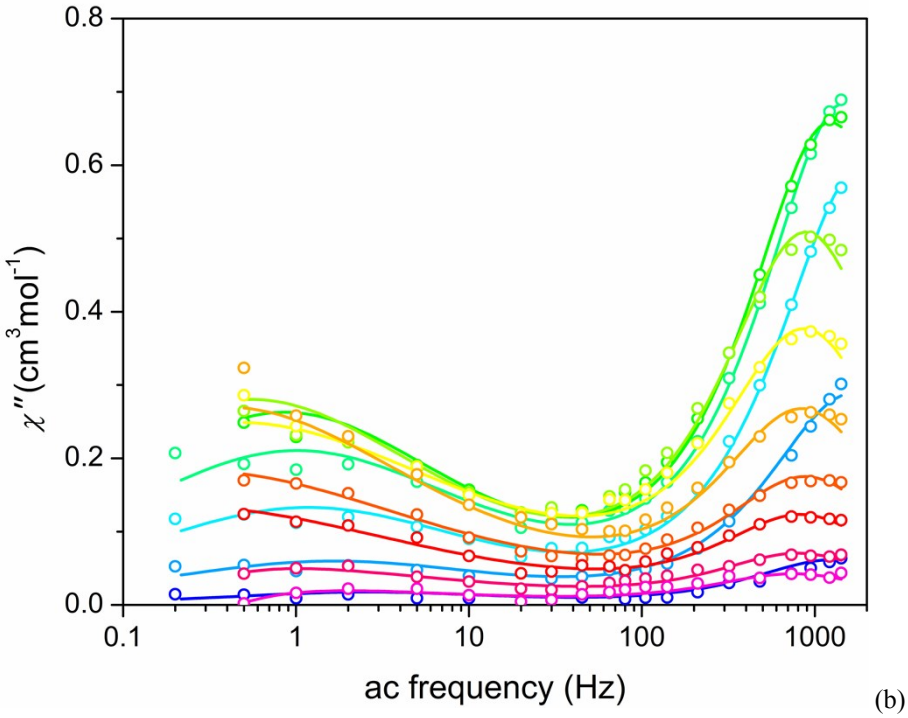

(b)

Figure S7. Frequency dependence of ac susceptibility per mol of Tb for $Ca_{9.5}Tb_{0.5}(PO_4)_6(OH_{0.75-\delta})_2$ under different magnetic fields at T = 1.8 K. (a) – in-phase susceptibility χ', (b) – out-of-phase susceptibility χ''. Symbols – experimental points, lines – fitting. The color designation: from blue to magenta – under a field of 0.3, 0.6, 1, 1.5, 2, 3, 3.5, 4, 5, 6, 8, 10 kOe respectively.

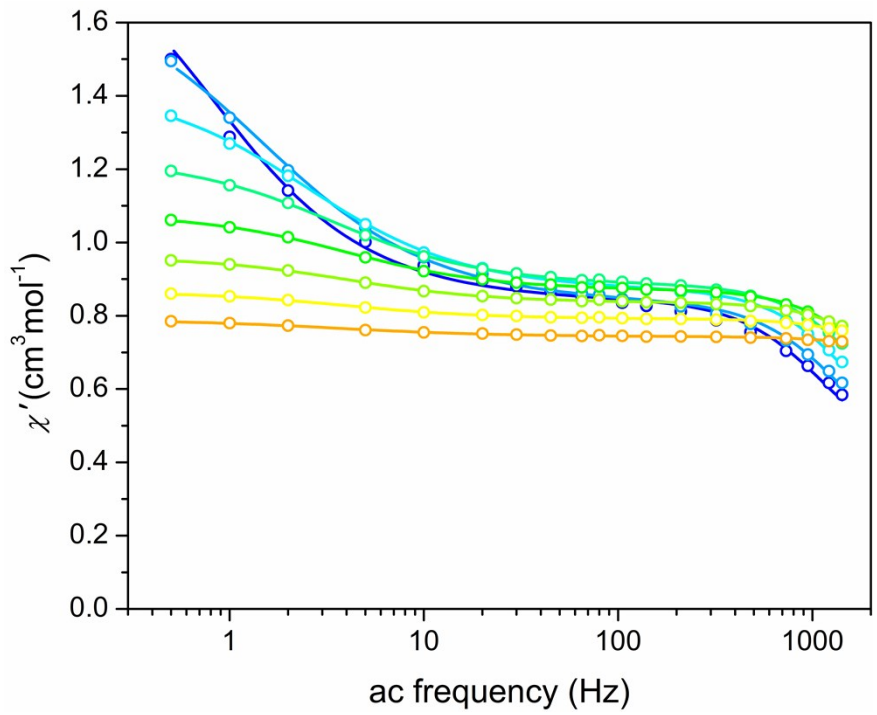

(a)

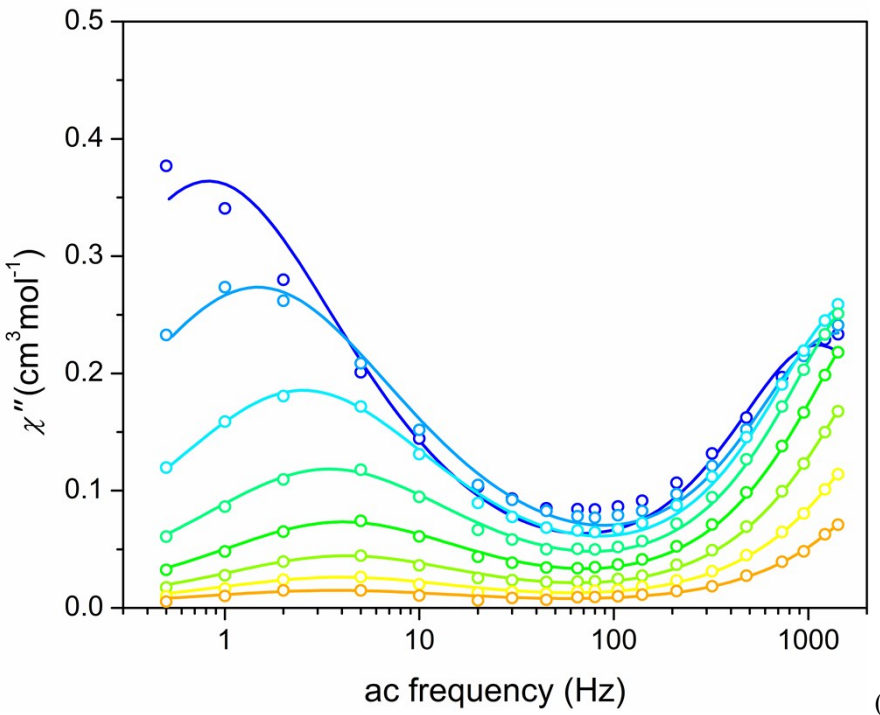

(b)

Figure S8. Frequency dependence of ac susceptibility per mol of Tb for $Ca_{9.5}Tb_{0.5}(PO_4)_6(OH_{0.75-\delta})_2$ at different temperatures under a field of 4 kOe. (a) – in-phase susceptibility χ', (b) – out-of-phase susceptibility χ''. Symbols – experimental points, lines – fitting. The color designation: from blue to orange – at T = 3, 4, 5, 6, 7, 8, 9, 10 K respectively.

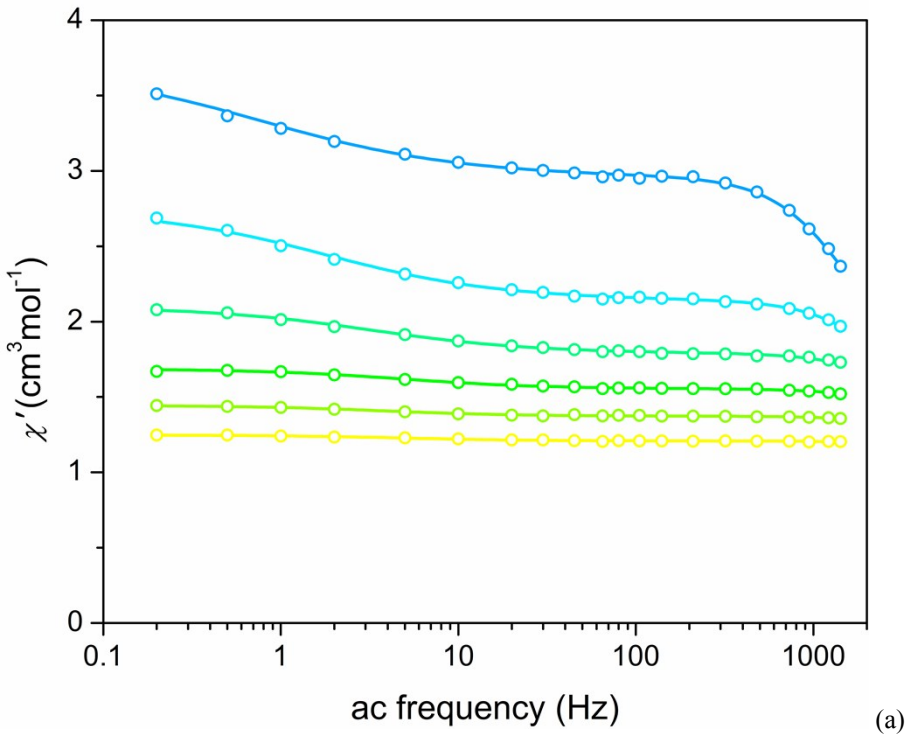

(a)

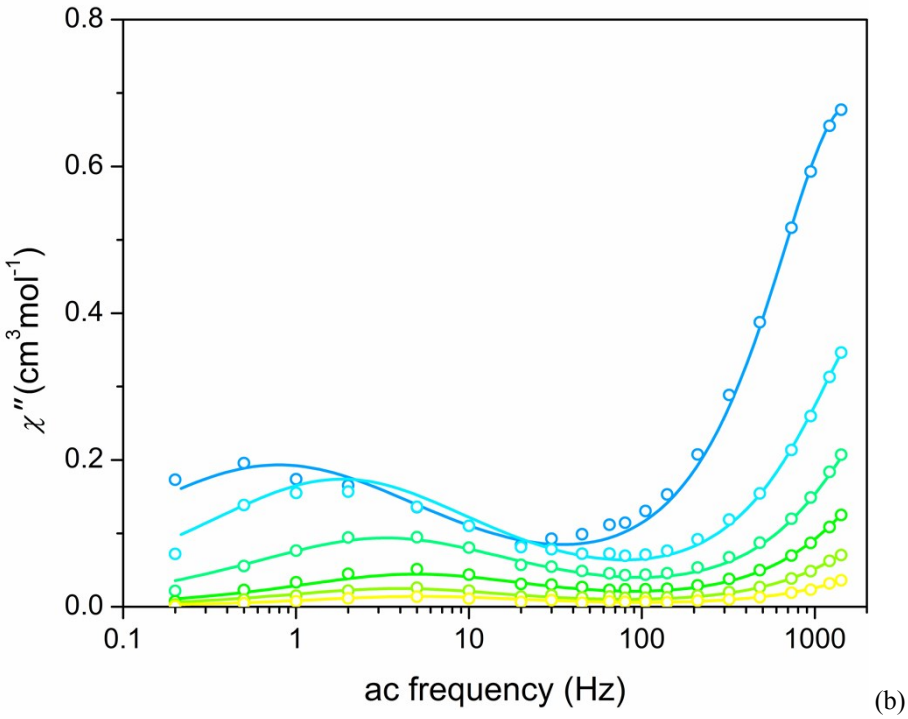

(b)

Figure S9. Frequency dependence of ac susceptibility per mol of Tb for $Ca_{9.5}Tb_{0.5}(PO_4)_6(OH_{0.75-\delta})_2$ at different temperatures under a field of 1.5 kOe. (a) – in-phase susceptibility χ', (b) – out-of-phase susceptibility χ''. Symbols – experimental points, lines – fitting. The color designation: from cyan to yellow – at T = 2, 3, 4, 5, 6, 7 K respectively.

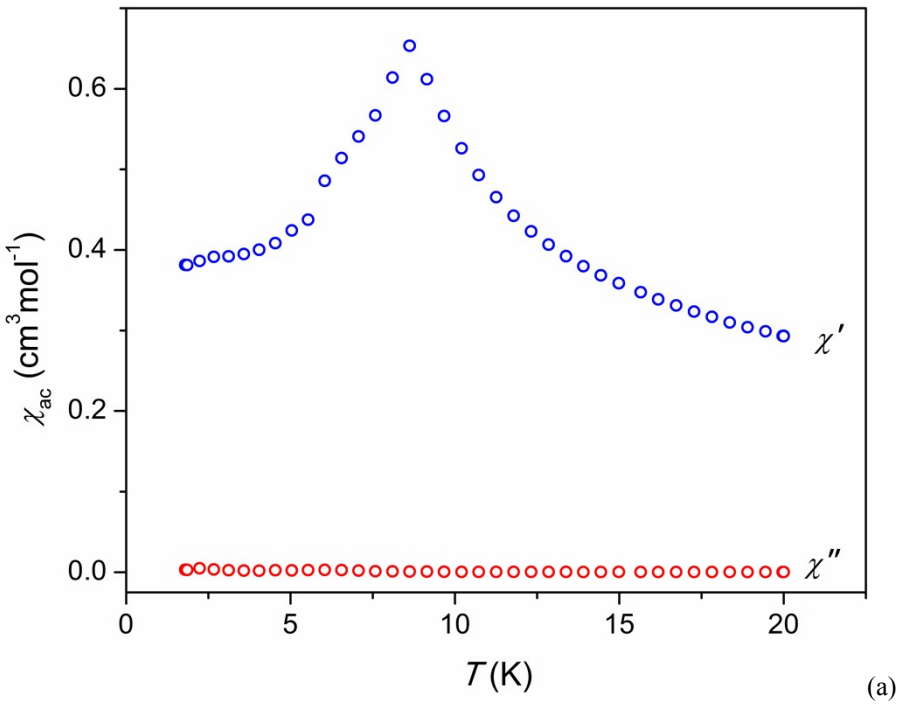

(a)

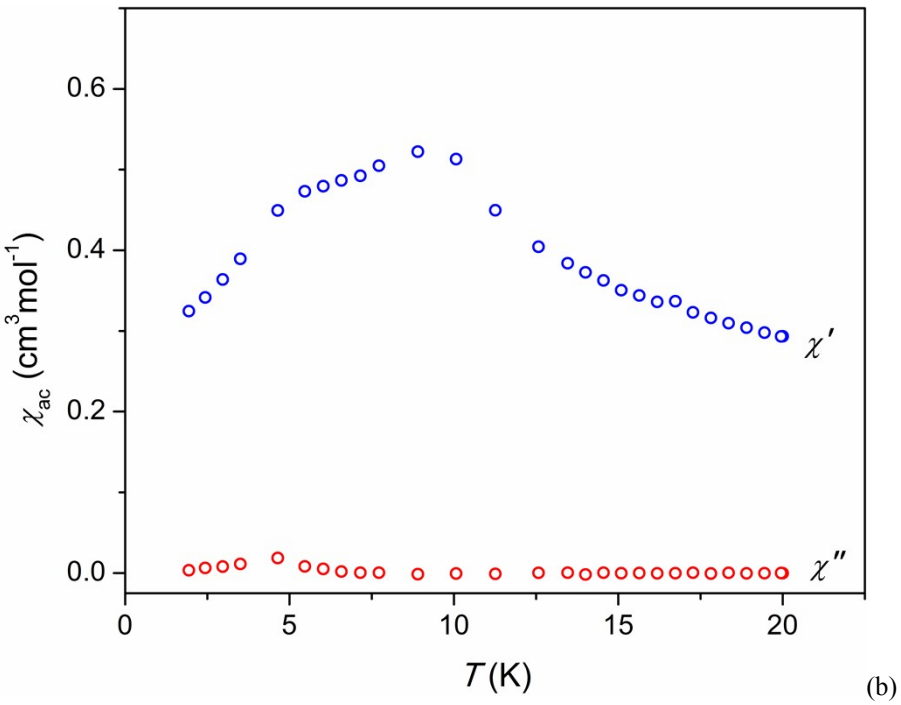

(b)

Figure S10. Temperature dependence of ac susceptibility per mol of Tb for Tb_4O_7 at an ac frequency of 80 Hz. (a) under a zero dc field, (b) under a field of 4 kOe.

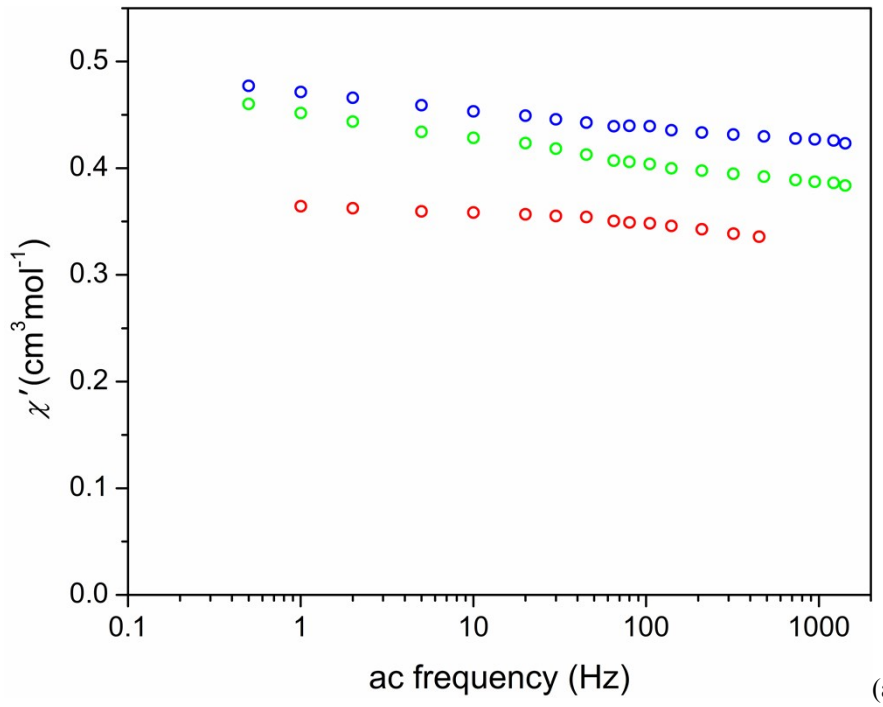

(a)

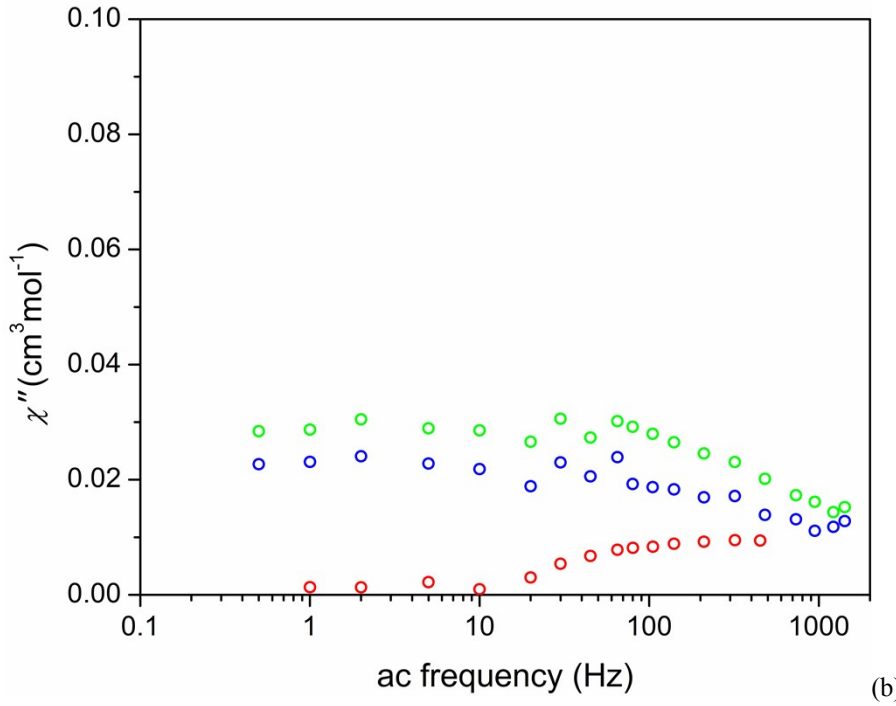

(b)

Figure S11. Frequency dependence of ac susceptibility per mol of Tb for Tb_4O_7 under different magnetic fields at T = 1.8 K. (a) – in-phase susceptibility χ', (b) – out-of-phase susceptibility χ''. The color designation: blue, green, and red – under a field of 1.5, 4, and 10 kOe respectively.